Open Access

Research on High Voltage Power for 10kV Linked SVG

Wang Huadong[*] and Cai Xu

Electronic Information and Electrical Engineering, Electrical Engineering, Shanghai Jiaotong University, Shanghai, China

Abstract: 10kV linked SVG module power supply from their own h-bridge power, supply is unstable. To solve this problem, this paper proposes a new way to take power, using a combination of full-bridge push-pull circuit with isolation transformer to solve the logical drive power between the power module and the SVG device self-consistent problem. The paper detailed analysis of the working principle and characteristics of this new way to take power, and verified on prototype, present the experimental results.

Keywords: h-bridge output, high voltage isolation, IGBT power module, isolation transformer, SVG, take power.

1. INTRODUCTION

Static Synchronous Compensator STATCOM (also known as domestic SVG) is one of the core equipment FACTS (Flexible Alternative Current Transmission Systems). The system can quickly compensate reactive, and take effective governance for harmonics, voltage fluctuations and flicker and other power quality problems, improve the safety and reliability of the system [1-3].

With the limits of the IGBT can withstand voltage level, current high voltage SVG module cascading is usually used as the main circuit topology, so require a separate power supply to drive IGBT for each module. Document 1 adopted high pulse transformers, high-voltage insulated wire, high-frequency current transformers, rectifiers and other design of a high-voltage isolation multiple low-voltage DC power supply, with too many components, the reliability is not high; Document 2 design a parallel high-voltage high-frequency isolated power bus, due to the use of high frequency bus, isolation transformers for special needs designed; Document 3 use the main power modules provide an AC bus to join rectifier, inverter and constitutes a multi-output isolation transformer isolated power supply, belong to the manner to take power from the H-bridge, likely to cause the transformer to burn out.

2. 10KV LINKED SVG PROGRAM

The overall structure of the chain of SVG 10kV main circuit is shown in Fig. (**1**), used Y-connector, ungrounded, access 10kV bus way through LCL. Controller is controlled by the signal conditioning boards with FPGA/DSP plates to power through the fiber-optic module sends instructions or

read the power module status. Power module consists of an h-bridge voltage source inverter and bypass, and bypass is used in case of inverter failure, short-circuit the output of the inverter, make chain of the inverter can still run properly, to achieve power redundancy module. Controller and power module provide DC power in the programs; the controller uses 24V power directly, the internal uses DC / DC circuits to generate the required voltage, e to implement easily. As the main circuit's neutral point ungrounded, power module housing may carry high voltage, direct current power supply part of the power module is required to have high voltage isolation [4-8].

3. COMPARISON OF THE POWER MODULE POWER DESIGN APPROACH

The main methods currently used to take power IGBT power module is H-bridge DC capacitor take power and H-bridge output take power.

(1) H-bridge DC capacitor takes power

H-bridge DC capacitor take power shown in Fig. (**2**), for 10kV chain SVG, if grid voltage fluctuation is, the line voltage spikes up is

$$10 \times 1.1 \times \sqrt{2} = 15.554 \text{ kV}$$

Transformed into a star without neutral on each phase, the withstand voltage for each phase H-bridge is

$$15.554 / \sqrt{3} = 8.98 \text{ kV}$$

Paper designed 10kV chain SVG power module per phase 12 cascades, each level of the DC bus voltage is set at 800 volts, can provide the maximum of DC voltage 9.6kV. The 800V is the average of the DC capacitor voltage, coupled with the continuous charging and discharging the capacitor voltage ripple generated will reach 1200V. On this basis, DC/DC converters can choose MOSFET switch or
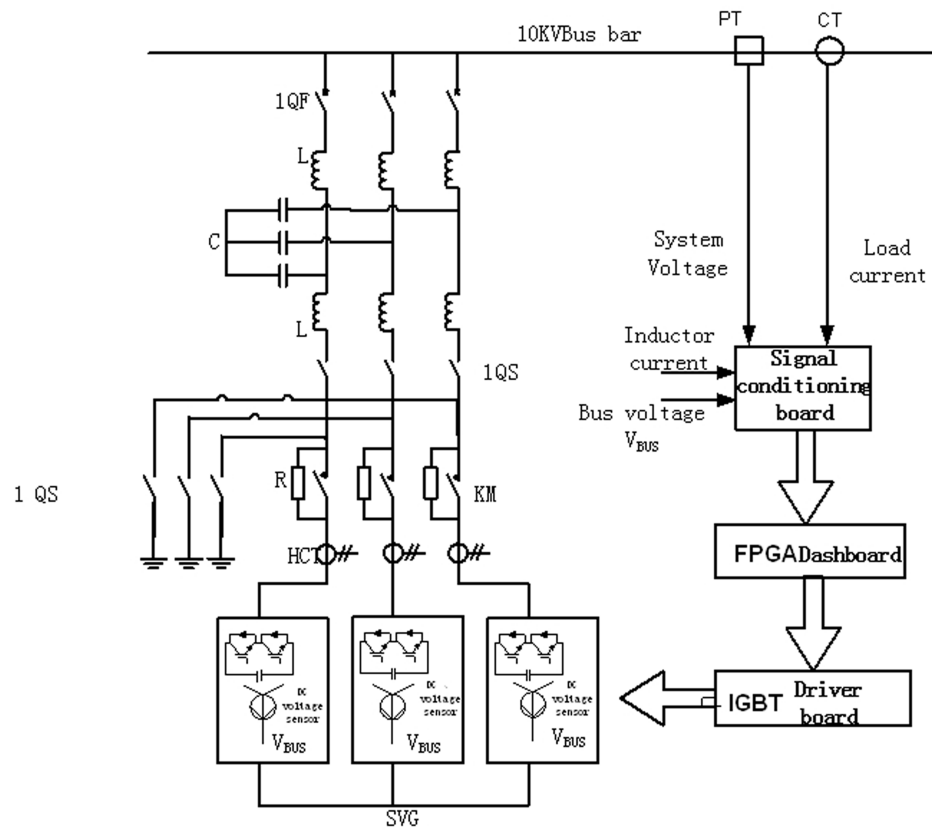
Fig. (1). 10kV chain SVG Chart.
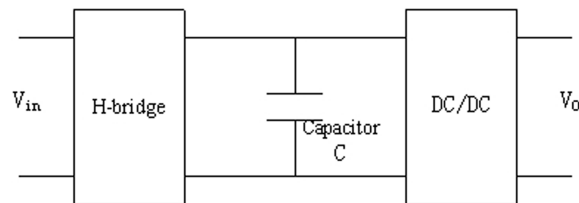
Fig. (2). Capacitor C take power.
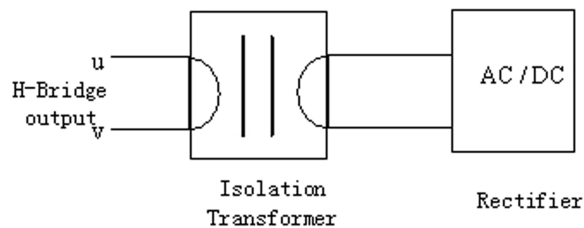
 Fig. (3). H-bridge output take power.

Bi-MOSFET. If MOSFET is chosen to be the switch, due to the current single MOS transistor can withstand voltages up to 1200V, requiring a two-stage MOS transistors connected in series in order to withstand the BUS voltage, and MOS transistors in series would involve grading, heat and a lot of other issues, reliability would become deteriorated. Bi-MOSFET can also be selected as a DC / DC switching tube, it is actually an IGBT, not a MOSFET, one level can be used, but the switching frequency is low, the cost is high, the volume is large, it is not practical [9, 10].

Therefore, the design approach is not suitable for 10kV chained SVG high voltage electrical source.

(2) H-bridge output take power

Fig. (**3**) is a way to take power though the outputs of h-bridge, which through isolation transformer insulation, takes
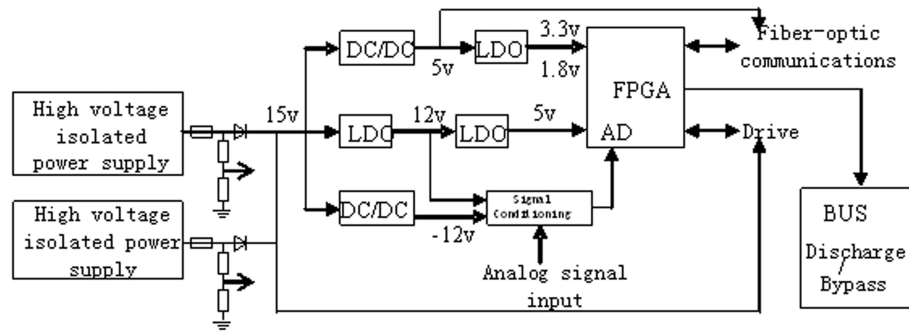
Fig. (4). Power Modules DC to take power structure diagram.
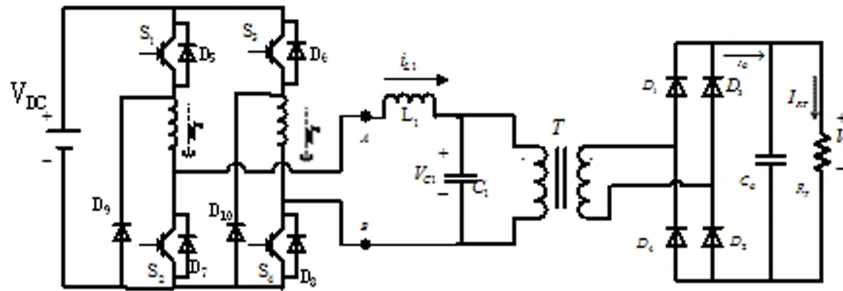
Fig. (5). High voltage isolated power supply topologies.

power with more reliability. However, there are the disadvantages:

(1) This method requires H-bridge output voltage stability, otherwise when the grid voltage is low (for low voltage ride through), H-bridge output voltage is too low to have the enough power output to drive IGBT;

(2) The H-bridge output is a square wave, input voltage distortion transformer is large, resulting in bulky, heavy, high harmonics serious loss;

(3) This approach requires a cascade of each transformer magnetizing inductance difference is small, otherwise when the machine starts, H-bridge has not been turned on, then quire the IGBT power cascade in 10kV power line, each isolation transformer combined to bear 10kV,if the transformer magnetizing inductance differences is large, may occur a cascade transformer withstand overvoltage breakdown [10-12].

Therefore, this scheme does not apply to 10kV chain SVG power module DC power to take power.

4. POWER MODULE HIGH VOLTAGE ISOLATED POWER DESIGN

Because STACOM controller (DSP, FPGA, CPLD and other control devices) require low-voltage DC power supply, so the devices typically need to be used as a secondary low-voltage DC power supply through the mains *via* a power converter, so this paper research is a new way to take power: integrated design with mode controller to take power, unified

to take power from low voltage direct current from the power supply (typically 24V) [13-17]. Wherein the overall design of the power supply module is shown in Fig. (**4**). IGBT driving voltage is 15V, directly from the isolated high pressure source, the other voltage levels can be obtained through the internal DC / DC conversion.

The internal structure of the high voltage isolation as shown in Fig. (**5**), which is a push-pull converted current source circuit, wherein s1, s2, s3, s4, L1, V1 constitutes the zero-current switching DC/AC conversion circuit, T is the isolation transformer, D1, D2, D3, D4 form a full-wave rectifier circuit.

The working process of a high voltage isolated power cycle can be divided into 12 stages, as shown in Fig. (**6**), since the phase of 7-12 and 1-6 is symmetry ,therefore the paper only analyzes the 1-6 stage.

Stage one: t1-t2

Power devices s3, s4 begins conducting at time t1, therefore at this stage is in the conducting state of the device with s1, s2, s3, s4, d3, d4, inductor L1releases the stored energy to the load, the current is iL1, the slope is vo/L1, when the inductor current becomes zero, the phase 1 ends, can obtain the following relationship:

$$v_{Cp}(t) = -V_O \tag{1}$$

$$i_{L1}(t) = \frac{V_O}{L_1}(t - t_1) - I_{LB} \tag{2}$$
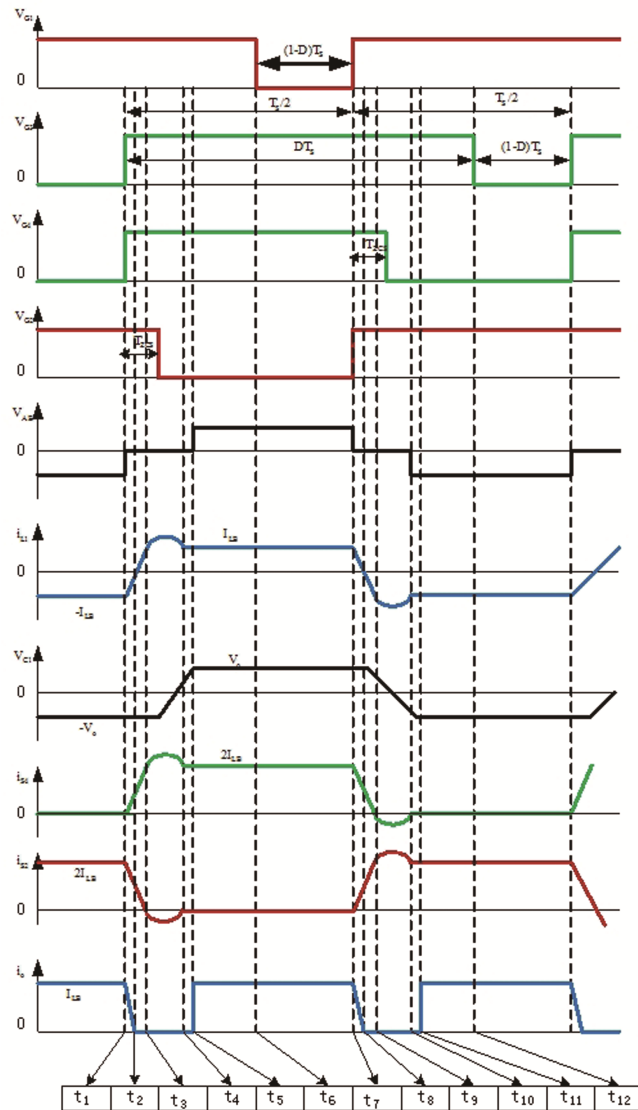
Fig. (6). High voltage isolated power one cycle timing diagram.

$$i_{S4}(t) = \frac{V_O}{L_1}(t - t_1) \tag{3}$$

$$i_{S2}(t) = 2I_{LB} - \frac{V_O}{L_1}(t - t_1) \tag{4}$$

$$i_O(t) = -i_{L1}(t) \tag{5}$$

The duration of Phase 1 can be obtained by the formula 2:

$$i_{L1}(t) = \frac{V_O\sqrt{C_1}}{\sqrt{L_1}}\sin(\frac{1}{\sqrt{L_1C_1}}(t - t_2)) \tag{6}$$

Stage two: t2-t3:

The inductor L1 current iL1 reduce to zero at the time t2, therefore the diode D3, D4 is off, only s1, s2, s3, s4 in the conduction state. The inductance L1 and the capacitor C1 begins to enter the series-resonance state, the current flowing through the inductor L_1 is

$$i_{L1}(t) = \frac{V_O\sqrt{C_1}}{\sqrt{L_1}}\sin(\frac{1}{\sqrt{L_1C_1}}(t - t_2)) \tag{7}$$

The current flows through S4 is

$$i_{S4}(t) = I_{LB} + \frac{V_O\sqrt{C_1}}{\sqrt{L_1}}\sin\left(\frac{1}{\sqrt{L_1C_1}}(t - t_2)\right) \tag{8}$$

The current flows through S2 is

$$i_{S2}(t) = I_{LB} - \frac{V_O\sqrt{C_1}}{\sqrt{L_1}}\sin(\frac{1}{\sqrt{L_1C_1}}(t - t_2)) \tag{9}$$
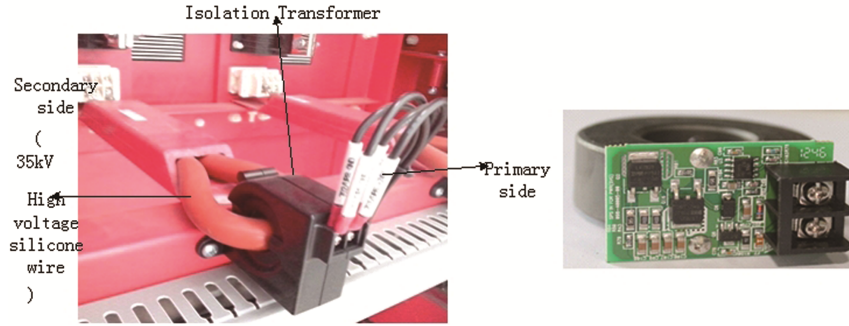
Fig. (7). Isolation high-voltage power supply experimental platform and circuit physical map.

The voltage on the capacitor C1 is

$$v_{C1}(t) = -V_o \cos\left(\frac{1}{\sqrt{L_1 C_1}}(t - t_2)\right) \tag{10}$$

The current of inductor L1is equal with ILB at the time t3, the duration of second phase can be obtained though the formula 7

$$T_{32} = t_3 - t_2 = \sqrt{L_1 C_1} \sin^{-1}\left(\frac{I_{LB}\sqrt{L_1}}{V_O\sqrt{C_1}}\right) \tag{11}$$

Stage three: t3-t4:

At this stage, S1, S3, S4 maintain the state, at t3, the anti-parallel diode D7 is turned on, the current in the inductor L1is at the maximum IP greater than ILB, achieve the zero current to shutdown S2,

$$I_p = |i_{L1}(t)|_{max} = \frac{V_O\sqrt{C_1}}{\sqrt{L_1}} \geq I_{LB} \tag{12}$$

The current of the inductor L1 drops to I_{LB} at time t4, L1 and C1 constitutes the series resonance state end. Its duration time is

$$T_{42} = \frac{\pi - \frac{1}{\sqrt{L_1 C_1}} T_{32}}{\frac{1}{\sqrt{L_1 C_1}}} = \pi\sqrt{L_1 C_1} - T_{32} \tag{13}$$

Stage four: t4-t5:

Stage of the switch status is consistent with stage 3 devices, the current of inductor L1is equal to IL1 and ILB, capacitor C1 start charging. The voltages on the capacitor C1 is:

$$v_{C1}(t) = v_{C1}(T_{42}) + \frac{I_{LB}}{C_1}(t - t_4) \tag{14}$$

The current flows through the switching device S4 is:

$$i_{S4}(t) = 2I_{LB} \tag{15}$$

The charging process is ended when the voltage of the capacitor C1 reaches Vo, diodes D1, D2 starts conducting. The time of the charging of the capacitor C1 can be represented with formula (16):

$$T_{54} = t_5 - t_4 = \frac{V_O\left(1 + \cos\left(\frac{1}{\sqrt{L_1 C_1}} T_{42}\right)\right)C_1}{I_{LB}} \tag{16}$$

Stage five: t5-t6:

The switching device with S1, S3, S4, D1, and D2 is in the conductive state, the power supply to the load, the voltage on the capacitor C1 is Vo, the output current io is ILB.

Stage six: t6-t7:

The S1 is turned off at the t6 time, the diode D9 is turned on, so that the switching device with S3, S4, D9, D1, and D2 is in the conducting state, the energy stored in the inductor L1 to supply power to the load. In this case the voltage on the capacitor C1 is Vo, the output current is ILB.

DC output voltage Vo can be obtained by the above analysis

$$V_O = \frac{2DV_{IN}}{1 - \frac{f_s}{f_r}\left(\begin{array}{c} 1 + \frac{P_O}{4\pi I_p DV_{IN}} - \frac{1}{\pi}\sin^{-1}\left(\frac{P_O}{2I_p DV_{IN}}\right) \\ + \frac{2I_p DV_{IN}}{\pi P_O}\left(1 - \sqrt{1 - \left(\frac{P_O}{2I_p DV_{IN}}\right)^2}\right) \end{array}\right)} \tag{17}$$

f_s is the switching frequency, $f_r = \frac{1}{2\pi\sqrt{L_k C_p}}$ is L1、 C1

series resonant frequency.

From equation (17) can be seen to achieve the control of output voltage Vo can adjust the duty cycle of the switching frequency.

5. PROTOTYPE RESULTS

To verify the correctness of the design, conducted experiments in the experimental device 10kV chain SVG, Vdc=24V, Vo=15V, Po=100W, Fig. (7) shows the
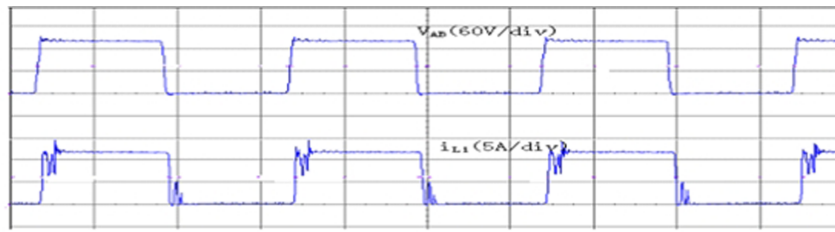
Fig. (8). VAB and the current IL1 of the inductance L1 waveform.
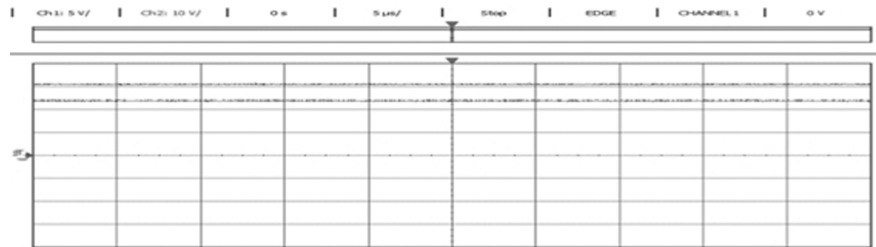
Fig. (9). 15V DC voltage output.
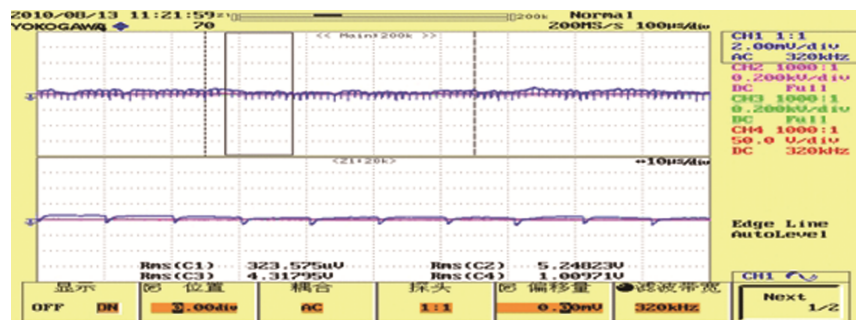
Fig. (10). DC 15V ripple voltage.

high-voltage isolation power supply experimental platform and circuit physical map, isolation transformer primary side using ordinary low voltage lines, isolation transformer secondary side has to stand high field strength caused by inhomogeneous electric field strength of the high pressure environment. Therefore, isolation transformer secondary side using 35kV high voltage silicone wire, cores connected to the ground [18-20]. Fig. (**8**) is a VAB and inductor L1 current IL1's waveform, it can be seen from the figure that the voltage and current to keep pace without delay lag. Fig. (**9**) is a 15V output voltage waveform, Fig. (**10**) is a DC 15V output ripple voltage, it can be seen from the figure that the maximum ripple voltage fluctuation is less than 1mv.

(1) 15V voltage switching cycle

(2) 15V output

(3)15V ripple voltage

10kV linked SVG will produce a lot of heat in the work process, making different high voltage isolation of electricity source at work environment temperature, high voltage isolation is easily affected by the temperature part that is the power isolation transformers, To verify paper designed applicability of the high voltage power supply in the case of different temperature, isolation transformer magnetizing current separately at room temperature and at 100℃ to take the test, the excitation current waveform is shown in Fig. (**11**) and Fig. (**12**) from the figure it can be seen that the excitation current has almost no change.

6. EPILOGUES

Thesis uses 10kV chain SVG power module as the way to take power for the study, developed a new way to take power. Take the controller and electric power modules into consideration, take 24V DC mains transformed as a power source, designed power module power conversion circuit, analyzes its working principle and characteristics, take the prototype produced, and the experiment and the experimental results confirm the correctness of the design.
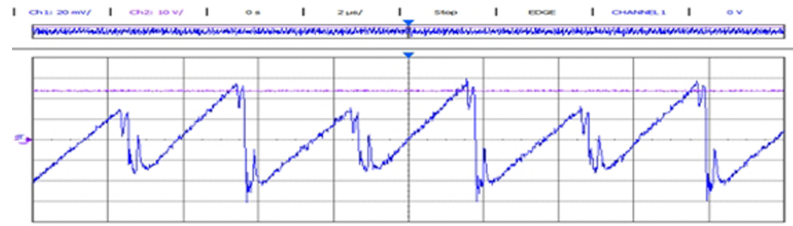
Fig. (11). Isolation transformer magnetizing current at room temperature.
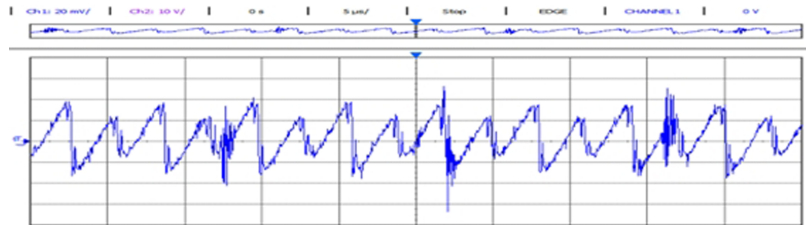
Fig. (12). Under 100 °C isolation transformer magnetizing current.

CONFLICT OF INTEREST

The authors confirm that this article content has no conflict of interest.

ACKNOWLEDGEMENTS

Declared none.

REFERENCES

[1]   Z. Qiushan, F. Dongqing, and L. Yi, "High-voltage isolation multichannel voltage DC power supply", *Electric Power Automation Equipment*, vol. 30, no. 1, pp. 136-144, 2010.

[2]   H. Yue, "*30kV Adjustable High-Voltage DC Power Supply Design*", Master Thesis, Dalian University of Technology, 2011.

[3]   J. Cunbo, X. Chunlei, C. Lihong, and W. Xile, "Design of high-isolation DC power supply for the cascaded high voltage pulse power", In: *5th International Conference on intelligent Human-Machine Systems and Cybernetics*, 2013, pp. 580-583.

[4]   C. Kaijiang, X. Yue, W. Guangning, X. Huihui, Z. Yiqiang, and L. Yang, "Insulation life model and partial discharge characteristic of magnet wires under square pulse voltage", *Journal of Southwest Jiaotong University*, vol. 47, pp. 626-634, 2012.

[5]   L. Xingqiao, T. Shaoqin, Z. Yongjian, C. Li, and L. Guohai, "The new zero-current PWM Full-BridgeDC-DC Converters", *Translations of Southeast University*, vol. 38, no. 2, pp. 58-61, 2008.

[6]   Z. Zheng, Z. Rongxiang, and Y. Huan, "Isolating transformers for reduced-order model of the inverter and synovial membrane of variable structure control", *Automation of Electric Power Systems,* vol. 36, no. 3, pp. 47-53, 2012.

[7]   B. Chuang, X. Yong, Z. Qian, and W. Jingmei, "BUCK ZCS PWM. converter of nonlinear dynamics", *Translations of System Simulation,* vol. 26, no. 3, pp. 710-725, 2014.

[8]   B. Basak, and S. Parui, "Exploration of bifurcation and chaos in buckconverter supplied from a rectifier", *IEEE Transactions on Power Electronics*, vol. 25, no. 6, 1556-1564, 2010.

[9]   Z. Xu, M. Li, F. Wang, and Z. Liang, "Investigation of Si IGBT operation at 200 °C for traction applications," *IEEE Transactions on Power Electronics*, vol. 28, no. 5, pp. 2604-2615, 2013.

[10]   G. Chen, Y. Wang, X. Cai, and S. Igarashi, "Adaptive digital drive for high power and voltage IGBT in multi-MW wind power converter," In: *Proceedings of IEEE Power Electronics and Motion Control Conference,* 2012, pp. 1452-1456.

[11]   M. A. Rodrìguez-Blanco, A. Claudio-Sànchez, D. Theilliol, L. G. Vela-Valdés, P. Sibaja-Ter´an, L.Hern´andez-Gonz´alez, and J. Aguayo-Alquicira, "A failure-detection strategy for IGBT based on gate-voltage behavior applied to a motor drive system," *IEEE Transactions on Industrial Electronics,* vol. 58, no. 5, pp. 1625-1633, 2011.

[12]   N. Gao, Y. Wang, X. Cai, and S. Igarashi, "Self-adaptivemultistage IGBT drivingmethod in medium voltagewind generation system," In: *Proceedings of IEEE Power Electronics and Motion Control Conference,* 2012, pp. 2287-2289.

[13]   B. S. Chen, and Y. –Y. Hsu, "A minimal harmonic control for a STATCOM", *Industrial Electronics*, vol. 55, no. 2, pp. 655-664, 2008.

[14]   B. Singh, S. S. Murthy, and S. Gupta, "Analysis and design of STATCOM-based voltage regulator for self-excited induction generators", *IEEE Power & Energy Society*, vol. 19, no. 4, pp. 783-790, 2004.

[15]   A. Yazdani, H. Sepahvand, and M. L. Crow, "Fault detection and mitigation in multilevel converter STATCOMs", *IEEE Industrial Electronics Society*, vol. 58, no. 4, pp. 1307-1315, 2011.

[16]   B. Ying, and Q. Chang, "A comparison of diode clamped and cascaded multilevel converter for a STATCOM with energy storage", *IEEE Transaction on Industry Electronics,* vol. 53, no. 5, pp. 1512-1521, 2006.

[17]   M. Noroozian, and N. A. Petersson, and B. Thorvaldson, "Benefits of SVC and STATCOM for electric utility application", In: *Transmission and Distribution Conference and Exposition Atlanta, USA,* 2003, pp. 957-958.

[18]   B. N. Singh, A. Chandra, and K. Al-Haddad, "DSP-based indirect-current-controlled STATCOM. II. Multifunctional capabilities", *Electric Power Applications,* vol. 147, no. 2, pp. 113-118, 2000.

[19]   Y. L. Tan, "Analysis of line compensation by shunt-connected FACTS controllers: a comparison between SVC and STATCOM" *Power Engineering Review*, vol. 19, no. 8, pp. 57-58, 1999.

[20]   P. W. Lehn, and M. R. Iravani, "Experimental evaluation of STATCOM closed loop dynamics", *IEEE Transactions on Power Delivery*, vol. 13, no. 4, pp. 1378-1384, 1998.